Bias dependence of tunneling magnetoresistance in magnetic tunnel junctions with asymmetric barriers

2013 J. Phys.: Condens. Matter 25 496005

(http://iopscience.iop.org/0953-8984/25/49/496005)

J. Phys.: Condens. Matter **25** (2013) 496005 (8pp) doi:10.1088/0953-8984/25/49/496005

Bias dependence of tunneling magnetoresistance in magnetic tunnel junctions with asymmetric barriers

Alan Kalitsov[1], Pierre-Jean Zermatten[2], Frédéric Bonell[3], Gilles Gaudin[2], Stéphane Andrieu[3], Coriolan Tiusan[3,4], Mairbek Chshiev[2] and Julian P Velev[1,2,5]

[1] Department of Physics, Institute for Functional Nanomaterials, University of Puerto Rico, San Juan, PR 00931, USA
[2] SPINTEC, UMR (8191) CEA/CNRS/UJF-Grenoble 1/Grenoble INP, INAC, 17 rue des Martyrs, F-38054 Grenoble Cedex, France
[3] Institut Jean Lamour, UMR 7198, CNRS-Nancy Université, BP 239, F-5406 Vandoeuvre, France
[4] Centre for Superconductivity, Spintronics and Surface Science (C4S), Technical University of Cluj-Napoca, Str. Memorandumului nr. 28, 400114 Cluj-Napoca, Romania
[5] Department of Physics and Astronomy, Nebraska Center for Materials and Nanoscience, University of Nebraska, Lincoln, NE 68588, USA

E-mail: kalitsov@yahoo.com and jvelev@gmail.com

Received 8 July 2013, in final form 10 October 2013
Published 6 November 2013
Online at stacks.iop.org/JPhysCM/25/496005

Abstract
The transport properties of magnetic tunnel junctions (MTJs) are very sensitive to interface modifications. In this work we investigate both experimentally and theoretically the effect of asymmetric barrier modifications on the bias dependence of tunneling magnetoresistance (TMR) in single crystal Fe/MgO-based MTJs with (i) one crystalline and one rough interface, and (ii) with a monolayer of O deposited at the crystalline interface. In both cases we observe an asymmetric bias dependence of TMR and a reversal of its sign at large bias. We propose a general model to explain the bias dependence in these and similar systems reported earlier. The model predicts the existence of two distinct TMR regimes: (i) a tunneling regime when the interface is modified with layers of a different insulator, and (ii) a resonant regime when thin metallic layers are inserted at the interface. We demonstrate that in the tunneling regime, negative TMR is due to the high voltage which overcomes the exchange splitting in the electrodes, while the asymmetric bias dependence of TMR is due to the interface transmission probabilities. In the resonant regime, inversion of TMR could happen at zero voltage depending on the alignment of the resonance levels with the Fermi surfaces of the electrodes. Moreover, the model predicts a regime in which TMR has different signs at positive and negative bias, suggesting possibilities of combining memory with logic functions.

(Some figures may appear in colour only in the online journal)

1. Introduction

The field of spintronics has been very successful in producing magnetoresistive devices for magnetic memory and sensor applications [1]. Magnetic tunnel junctions (MTJs) came to the forefront of spintronics research after theoretical predictions of very high positive tunneling magnetoresistance (TMR) in Fe/MgO/Fe MTJs [2]. Shortly after, TMR in excess of 200% was reported experimentally in these junctions [3, 4]. More recently TMR as high as 604% at room temperature was reported in MgO-based MTJs with CoFeB electrodes [5]. It has been recognized that the interfaces are crucial for

the TMR amplitude and voltage dependence, and consequently interface engineering has received a great deal of attention [6, 7].

There are a number of experimental studies of the influence of modified interfaces on the sign and bias dependence of TMR, in particular with insulating layers such as Ta_2O_5 [8] and NiO [9], metallic layers Cr [10] and Fe_3O_4 [11], adatoms C [12, 13] and O [14, 15], and morphologically different interfaces [16–19]. A recent experimental work shows that the insertion of a thin NiO layer at one of the interfaces of a CoFe/MgO/CoFe(001) MTJ gives rise to an asymmetric bias dependence of the TMR [9]. Also, switching from positive to negative TMR was observed at larger bias. It was suggested that the effect is due to formation of a non-collinear magnetic structure at the CoFe/NiO interface, however, it is not clear how that fact may affect the bias dependence of TMR. Very similar observations were reported earlier in NiFe/Ta_2O_5/Al_2O_3/NiFe MTJs [8]. The sign reversal was interpreted, using the Jullière model, in terms of the change of the spin polarization of the electrodes with the bias [20]. Strongly asymmetric TMR bias dependence was also reported. Moreover, essentially identical behavior and sign reversal of TMR was observed in experiments doping the interface with non-magnetic metal layers (Cr) [10], non-magnetic atoms (C) [12, 13], or by just varying the morphology of the interface [16].

First principles transport calculations with finite bias are fairly difficult and therefore not commonplace. There are several density functional theory based calculations of Fe/MgO-based MTJs with ideal and oxidized interfaces at finite bias [18, 21–24]. Some of them consider MTJs with asymmetrically modified interfaces and report asymmetric behavior of TMR [18, 20, 23]. Overall, the asymmetric bias dependence and sign change of TMR emerge as general features of many diverse systems, however, interpretation is usually limited to qualitative arguments based on the Jullière model on a case-by-case basis. Further analysis is needed to understand the underlying physics of these phenomena.

In this paper, we report measurements of the bias dependence of TMR in pairs of single crystal Fe/MgO MTJs—one with clean interfaces (Fe//MgO/Fe) and another with a monolayer of O deposited at one of the interfaces (Fe/O/MgO/Fe). Due to the growth procedure, in both cases the bottom (first) interface is atomically sharp while the top (second) is of lower quality [25]. The experiments show that TMR is asymmetric with respect to the voltage sign and negative TMR arises at high voltage. The insertion of an O layer at the higher quality interface acts as an additional barrier and slightly reduces the asymmetry of the bias dependence of TMR [14, 25]. We propose a model which explains these experimental observations as well as other previously reported experiments. The model relates the interface asymmetry to the interface transmission functions. We show that interface modifications which preserve the tunneling regime lead to asymmetric bias dependence and TMR inversion at large bias, while modifications with metallic layers can lead to TMR inversion even at zero bias due to resonant transmission.

2. Experimental results

The details of the experimental procedure have already been discussed in previous papers [14, 17]. The samples were grown on MgO(001) substrate and the MgO barrier thickness was between 1.1 and 2.3 nm (5–11 monolayers). Pairs of samples, Fe//MgO/Fe (A) and Fe/O/MgO/Fe (B), were grown simultaneously by molecular beam epitaxy in the same ultra-high vacuum (UHV) chamber (base pressure less than 10^{-10} Torr). After the deposition of the bottom Fe(001) electrode on both samples, sample A was put into a secondary UHV chamber, adjacent to the growth chamber. Then, molecular O was adsorbed at room temperature on the bottom Fe surface of sample B only. The deposition was stopped after adsorption of one O monolayer. The O adsorption was controlled in real time *in situ* by x-ray photoelectron spectroscopy (XPS) as described in detail in the previous work [14]. Then, both samples were annealed at 925 K. In sample B, the annealing resulted in $p(1 \times 1)$ ordering of the adsorbed O monolayer. Subsequently the MgO barrier and the top Fe layer were grown. The MgO barrier growth was not affected by the presence of the O layer which was confirmed by observing the RHEED pattern during the barrier deposition [14]. No annealing of the top electrode was performed in order to prevent any further evolution of the bottom interface with respect to the initial configuration. For this reason the second MgO/Fe interface is of lower quality. The most important feature of this procedure is that the thicknesses, growth and annealing conditions for both bottom Fe electrodes and the MgO barrier were strictly identical for both A and B samples. Therefore, the differences in the transport characteristics are only related to the presence of the additional O monolayer at the bottom Fe/MgO interface.

Measurements of the bias dependence of TMR were performed on both Fe//MgO/Fe and Fe/O/MgO/Fe MTJs for 1.1, 1.6 and 2.3 nm MgO barrier thickness. The currents $I_P = I_{\uparrow\uparrow} + I_{\downarrow\downarrow}$ and $I_{AP} = I_{\uparrow\downarrow} + I_{\downarrow\uparrow}$ are measured for magnetizations in the electrodes parallel (P) and antiparallel (AP) to each other. Then the TMR ratio is calculated as $\mathrm{TMR} = (I_P - I_{AP})/I_{AP}$. The bias dependence of the TMR in the sample with 1.1 nm of MgO barrier is shown in figure 1. The TMR curves for 1.6 and 2.3 nm are qualitatively similar except for a higher value of TMR and larger noise level. The noise increase with increasing thickness and/or decreasing bias is due to the smaller magnitude of the measured current, which leads to a decrease in precision. The maximum TMR value is obtained at small finite bias from where TMR monotonically decreases with the bias. A similar shift of the maximum to finite bias is observed in most asymmetric MTJs, for example with NiO [9], Fe_3O_4 [11] or C modified barriers [11, 25].

TMR increases with the thickness of the MgO barrier, with a maximum value of 50% for 1.1 nm, 117% for 1.6 nm and 142% for 2.3 nm for the MTJs with non-oxidized interfaces. The maximum TMR value obtained for the thicker MgO barrier is slightly lower than the ratio measured earlier [25], because in these samples the top Fe electrode has not been annealed and therefore the structural quality of the

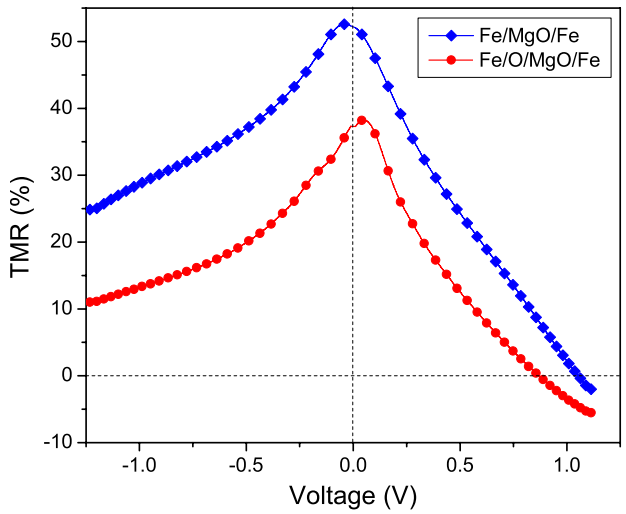

Figure 1. Experimental bias dependence of TMR in single crystal Fe/MgO/Fe and Fe/O/MgO/Fe MTJs. The thickness of the MgO barrier is 1.1 nm. The top Fe electrode is taken as reference while the bias is applied to the bottom Fe electrode. A numerical smoothing procedure is applied to reduce the experimental noise around zero bias.

MTJ stack is slightly reduced. Comparing samples A and B for the same MgO barrier, we observe that the presence of one monolayer of O at the bottom Fe/MgO interface decreases the TMR in all cases with respect to the O-free samples (to 38% for 1.1 nm, 50% for 1.6 nm, and 115% for 2.3 nm barriers, respectively). These observations are consistent with previous reports [2, 26, 27].

In all cases TMR is asymmetric with respect to the voltage. We also observe that TMR changes sign at large bias from positive to negative. Due to the asymmetry, the inversion happens only at positive bias for the experimental range of voltages, which is limited to prevent electric breakdown. In order to quantify and compare the TMR asymmetry between samples, we define V_+ and V_- to be the absolute values of the bias at which TMR reaches half of its maximum value for positive and negative bias, respectively. For the 1.1 nm thick MgO barrier (figure 1) with non-oxidized interfaces we obtain $V_+ = 0.42$ V and $V_- = 1.04$ V. We define an asymmetry coefficient as follows: $\gamma = |(V_+ - V_-)/V_-| = 60\%$. This asymmetry is large, suggesting that the quality of the two interfaces is markedly different. This is not surprising bearing in mind that the bottom Fe/MgO interface is atomically sharp after the annealing of the bottom Fe electrode, while the top MgO/Fe interface is rougher for a couple of reasons. First, the 1.1 nm MgO thickness is larger than the critical thickness for the pseudomorphic MgO growth on Fe above which plastic relaxation occurs [28], creating dislocations within the MgO. Second, the top Fe electrode is not annealed which reduces its morphological and crystallographic properties compared with the bottom one. The same measure for the oxidized sample gives $\gamma = 28\%$ ($V_+ = 0.29$ V and $V_- = 0.4$ V). Clearly, the O monolayer reduces the asymmetry of the bias dependence of the TMR.

Similarly, for the MTJs with 1.6 nm of MgO for the clean interface we obtain asymmetry of $\gamma = 69\%$ ($V_+ = 0.42$ V and $V_- = 1.37$ V), while again the oxidized interface makes TMR more symmetric $\gamma = 25\%$ ($V_+ = 0.41$ V and $V_- = 0.55$ V). A qualitatively similar asymmetry reduction was observed for the MTJs with 2.3 nm of MgO barrier. Thus, we can conclude that in the junction with clean interfaces, the two interfaces are of very different quality which leads to the strong asymmetric bias dependence of the TMR, consecutively leading to the inversion of the TMR at large positive bias when injecting towards the bottom atomically flat Fe/MgO interface. At the same time the presence of an O monolayer at this atomically flat Fe/MgO interface reduces the asymmetry of the TMR. Since the addition of the O monolayer does not qualitatively change the bias dependence of TMR its role can be understood simply as an additional barrier. The fact that the asymmetry is more or less the same for all thicknesses suggests that it is predominantly determined by the interfaces.

3. Model results

In order to gain more insight on how interface modifications affect the bias dependence of TMR we perform model calculations. We consider the standard two-probe setup, consisting of the scattering region (S) coupled to the left (L) and the right (R) ferromagnetic leads. Except that in our case, we further subdivide the scattering region into three different parts, $S = B_L|B|B_R$, corresponding to the parts adjacent to the left interface, in the middle and adjacent to the right interface, respectively. The electronic structure is described on the level of a single-orbital tight binding (TB) model. In the case of Fe/MgO-based MTJs, this model has predictive power due to the particular band structure of the ferromagnetic leads which can be thought to contain only one exchange-split Δ_1 band [29–36]. This model represents an approximation in a couple of ways: (i) it ignores the contribution to the transport of the bands with symmetries other than Δ_1 and (ii) it does not account for the contribution of the interface resonance state present in the minority Fe. For finite bias the rigid band approximation is used, i.e. that bands are rigidly shifted in energy by the applied bias. The voltage drop is entirely in the barrier region. We assume that the electrostatic potential changes linearly within the barrier. This model has been demonstrated previously to describe remarkably well the behavior, not only of the charge current and TMR behavior [29–31], but also of the spin current and the spin-transfer torque (STT) [32–36]. At the same time the model gives us the opportunity to readily calculate the voltage dependence of the current and TMR in MTJs with a variety of barrier modifications.

The Hamiltonian for the MTJ is

$$H = H_L + H_R + H_S + (H_{SL} + H_{SR} + \text{h.c.})$$

where the different terms represent the isolated left and right leads $H_{L(R)} = \sum \varepsilon_\lambda^\sigma c_\lambda^{\sigma\dagger} c_\lambda^\sigma + \sum t_{\lambda\mu} c_\lambda^{\sigma\dagger} c_\mu^\sigma$, the scattering region $H_S = \sum \varepsilon_i c_i^{\sigma\dagger} c_i^\sigma + \sum t_{ij} c_i^{\sigma\dagger} c_j^\sigma$ and the coupling between the leads with the scattering region $H_{SL(R)} = \sum t_{a\alpha(b\beta)} c_{a(b)}^{\sigma\dagger} c_{\alpha(\beta)}^\sigma$. By convention the first principal layers of the left (right) interface are labeled α (β) indices in the leads and a (b)

in the barrier. The spin-split Δ_1 bands in the Fe electrodes are represented by their spin-dependent onsite energies $\varepsilon^{\uparrow} = 3.0$ eV and $\varepsilon^{\downarrow} = 5.6$ eV respectively. The onsite energy in the bulk MgO barrier is $\varepsilon_B = 9.0$ eV (B region). We vary the onsite energies in the B_L and B_R regions to model MTJs with modified interfaces. The nearest neighbor hopping matrix elements are chosen to be $t = -1.0$ eV in all regions. The Fermi energy is at $E_F = 0.0$ eV. The calculations were carried out at low temperature.

The finite bias tunneling current is calculated using the standard Landauer formalism [37, 38]

$$I_{\sigma\sigma'} = \frac{e}{h}\int \mathrm{d}E\,\mathrm{d}\boldsymbol{k}_{\parallel}\,[f(E,\mu_L) - f(E,\mu_R)]\,T_{\sigma\sigma'}(E,\boldsymbol{k}_{\parallel})$$

where the transmission probability $T_{\sigma\sigma'}\left(E,\boldsymbol{k}_{\parallel}\right) = \mathrm{Tr}[\Gamma_L^{\sigma} G^{\sigma\sigma'} \Gamma_R^{\sigma'} G^{\sigma\sigma'\dagger}]$ is integrated over $\boldsymbol{k}_{\parallel}$ in the surface Brillouin zone and over energy within the bias window. The bias window is controlled by the Fermi–Dirac distribution function f where $\mu_{L(R)}$ is the chemical potential in the L (R) lead. The retarded Green's function (GF) of the scattering region connected to the leads is $G^{\sigma\sigma'} = (g_S^{-1} - \Sigma_L^{\sigma} - \Sigma_R^{\sigma'})^{-1}$, where g_S is the GF of the isolated scattering region and $\Sigma_{L(R)}^{\sigma} = t_{a\alpha(b\beta)}^2 g_{L(R)}^{\sigma}$ is the self-energy associated with the connection to the electrodes. The escape rate to the electrodes $\Gamma_{L(R)}^{\sigma} = \mathrm{i}(\Sigma_{L(R)}^{\sigma} - \Sigma_{L(R)}^{\sigma\dagger}) = 2\pi t_{a\alpha(b\beta)}^2 \rho_{L(R)}^{\sigma}$ is proportional to the spin-dependent electrode surface density of states (DOS) $\rho_{L(R)}^{\sigma} = -\mathrm{Im}(g_{L(R)}^{\sigma})/\pi$. Within the single-band TB model and in the *limit of a thick barrier* [36], the transmission probability can be simplified to

$$T_{\sigma\sigma'}\left(E,\boldsymbol{k}_{\parallel}\right) = \frac{\Gamma_L^{\sigma}\Gamma_R^{\sigma'}|g_{ab}|^2}{|1 - g_{aa}\Sigma_L^{\sigma}|^2 |1 - g_{bb}\Sigma_R^{\sigma'}|^2}$$

where the assumption of a thick barrier allows for the multiple scattering terms in the denominator to be ignored. The interface transmission functions or probabilities (ITFs) can be expressed as $t_L^{\sigma} = (\Gamma_L^{\sigma}/t_{a\alpha})\left(1 - t_{a\alpha}^2 g_{aa}^2\right)/|1 - g_{aa}\Sigma_L^{\sigma}|^2$ and $t_R^{\sigma'} = (\Gamma_R^{\sigma'}/t_{b\beta})(1 - t_{b\beta}^2 g_{bb}^2)/|1 - g_{bb}\Sigma_R^{\sigma'}|^2$ by performing the wavefunction matching at each interface [39]. The ITFs have the meaning of the *induced* electrode DOS in the scattering region and can be written as a product of the electrode's surface DOS and a spin-dependent function of the barrier potential at the interface $t_{L(R)}^{\sigma} = \rho_{L(R)}^{\sigma} D_{L(R)}^{\sigma}$. Clearly in the limit of a very high barrier $g_{ii} \ll 1$ and the ITFs reduce to the electrode DOS, which is the Jullière limit. Using the ITFs we can express the transmission probability as

$$T_{\sigma\sigma'}\left(E,\boldsymbol{k}_{\parallel}\right) = t_L^{\sigma}|S_{ab}|^2 t_R^{\sigma'}$$

where S_{ab} can be interpreted as the matrix element of the scattering matrix across the barrier. This expression reduces to $T_{\sigma\sigma'} = t_L^{\sigma} \mathrm{e}^{-2\kappa d} t_R^{\sigma'}$, where κ is the decay constant in the barrier and d is the barrier thickness, at zero bias and a uniform barrier [40–42]. TMR can be expressed through the ITFs as follows:

$$\mathrm{TMR} = \frac{\int \mathrm{d}\varpi\,|S_{ab}|^2 (t_L^{\uparrow} t_R^{\uparrow} + t_L^{\downarrow} t_R^{\downarrow} - t_L^{\uparrow} t_R^{\downarrow} - t_L^{\downarrow} t_R^{\uparrow})}{\int \mathrm{d}\varpi\,|S_{ab}|^2 (t_L^{\uparrow} t_R^{\downarrow} + t_L^{\downarrow} t_R^{\uparrow})}$$

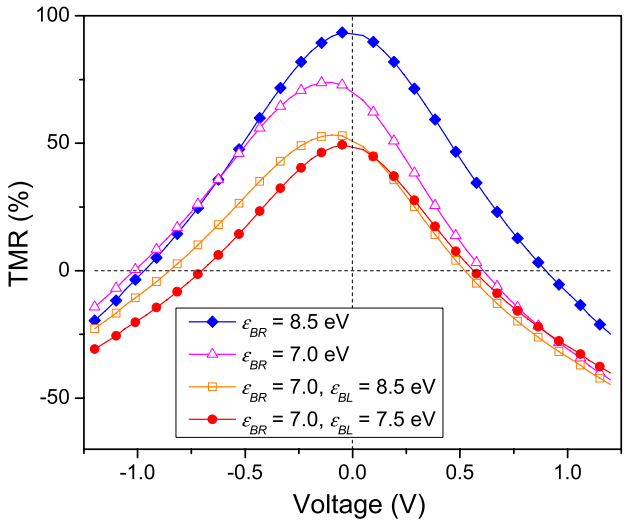

Figure 2. Calculated bias dependence of TMR in Fe/MgO/Fe and Fe/O/MgO/Fe MTJs. Oxygen in Fe/O/MgO/Fe MTJs is represented by 1 monolayer at the left interface with onsite energy ε_{B_L}. The rough right interface is represented with 1 monolayer with onsite energy ε_{B_R}. The thickness of the middle part of the MgO barrier is 4 monolayers.

where $\int \mathrm{d}\varpi = \int \mathrm{d}E \int \mathrm{d}\boldsymbol{k}_{\parallel}\,[f(E,\mu_L) - f(E,\mu_R)]$. At zero bias and at the Γ point only, it reduces to the familiar Jullière formula $\mathrm{TMR} = 2P_L P_R/(1 - P_L P_R)$, where $P_{L(R)} = (t_{L(R)}^{\uparrow} - t_{L(R)}^{\downarrow})/(t_{L(R)}^{\uparrow} + t_{L(R)}^{\downarrow})$ is the spin polarization of the DOS induced in the barrier by the electrodes.

Using this model we calculate the tunneling current and TMR in Fe/MgO/Fe MTJs corresponding to the experimental setup. For sample A we assume that at the sharp interface the barrier is identical to the bulk $\varepsilon_{B_L} = \varepsilon_B = 9.0$ eV, while at the rough interface the barrier height is reduced. We vary $6.0 < \varepsilon_{B_R} < 9.0$ eV, which still represents a barrier layer albeit smaller than the bulk. The calculated TMR as a function of the applied bias is shown in figure 2. It can be seen that when ε_{B_R} is close to the bulk value, the TMR is symmetric and close to the ideal case. As ε_{B_R} decreases, the maximum value of TMR decreases and the asymmetry is increased. Moreover, we see that for large enough bias TMR changes sign, but due to the asymmetry this inversion happens for much smaller bias in one direction than in the other. These results show qualitative agreement with the experimental observations. An asymmetry coefficient approximately equal to the experimental one is obtained for the value of $\varepsilon_{B_R} = 7.0$ eV. Thus, this model allows us to interpret many similar experiments in which one of the interfaces is morphologically different [16–19]. In those cases, disorder and roughness make the barrier at the interface more diffuse, effectively lowering the barrier height, which gives rise to asymmetric behavior.

Similarly, we calculate the bias dependence of the TMR in sample B, where we fix $\varepsilon_{B_R} = 7.0$ eV to account for the rough interface and vary the onsite energy of the O monolayer $7.0 < \varepsilon_{B_L} < 9.0$ eV. The results, plotted in figure 2, show that the asymmetry is reduced. The same asymmetry as in experiment ($\gamma = 28\%$ for 1.1 nm of MgO barrier) is obtained for $\varepsilon_{B_L} = 7.5$ eV. Thus, within our model, the O layer can be

understood as an additional barrier. This agrees well with the experimental observation that the O layer attenuates both the P and AP spin channels the same, which behavior is consistent with an additional barrier at the interface [14].

In the case when all parts of the barrier are insulating, the ITFs (t_L and t_R) are largely determined by the DOS at the electrodes. Thus, the decrease in TMR and the subsequent sign reversal at finite bias, for both symmetric and asymmetric MTJs, could be qualitatively explained in terms of the realignment of majority- and minority-spin DOS in the left and right electrodes [8]. The band alignments at zero and finite basis are illustrated in figure 3(a). At zero bias the majority and minority bands are aligned in the P configuration, and misaligned in the AP configuration (due to exchange splitting). The propagating states in the electrodes in the P configuration experience no scattering, while in the AP a large portion of the states is scattered. Thus, the majority channel in the P configuration ($I_{\uparrow\uparrow}$) dominates the current and TMR is positive ($I_P > I_{AP}$). Applied bias rigidly shifts the bands in the electrodes. The effect is that in the P configuration the bands get less and less aligned increasing the scattering and reducing I_P, while the alignment in the AP configuration improves. As a result I_{AP} increases faster with bias than I_P. At some bias the two channels become equal and TMR becomes negative ($I_P < I_{AP}$). This happens when the bias is comparable to the exchange splitting, aligning the majority and minority bands, in which case the transmission probability is dominated by one of the channels in the AP configuration ($I_{\downarrow\uparrow}$ for negative bias or $I_{\uparrow\downarrow}$ for positive bias).

For symmetric MTJs the bands in the P orientation at zero bias have an optimum alignment and no scattering. Thus any bias introduces some scattering and causes I_P to increase with bias slower than I_{AP}. In asymmetric MTJs, however, the ITFs at the two interfaces are not equal. The potential profiles of a barrier with an insulating layer of lower barrier height at the right interface are drawn in figure 3(b) for zero and finite bias. In this case $t_R > t_L$ and there is some scattering in the P channel even at zero bias. One of the effects of this is that TMR is lowered compared to the symmetric case because the P channel conduction is suboptimal. Applying negative bias decreases the effective barrier height at the left interface and increases it at the right interface. This will tend to decrease t_R and increase t_L, reducing the scattering the in the P channel and making I_P increase faster than I_{AP}. Positive bias works in the opposite direction. Thus, the second effect is that the TMR maximum switches to finite negative bias.

When the bias becomes comparable to the size of the barrier reduction at the right interface I_{AP} will again outpace I_P. However, since negative bias in general improves the alignment and reduces the scattering in the P configuration it will take larger negative bias, compared to the symmetric barrier, before $I_{AP} > I_P$ and TMR becomes negative. Positive bias does the opposite and smaller positive voltage is required to change the sign of TMR.

These observations allow us to generalize the model to explain experiments in which extra insulating layers are inserted at the interface, in particular NiFe/Ta_2O_5/Al_2O_3/NiFe [8] and CoFe/NiO/MgO/CoFe MTJs [10]. In both cases,

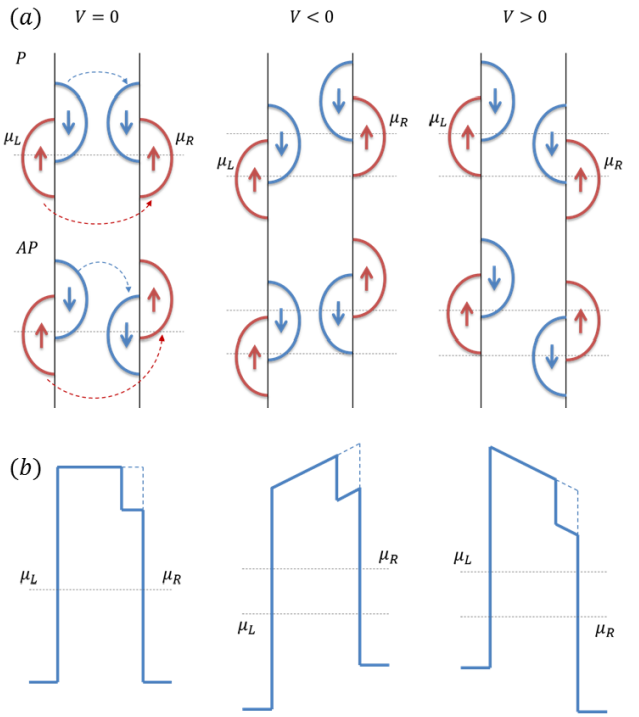

Figure 3. Schematic representation of the electronic structure of the electrodes and the barrier in an MTJ at different voltages. (a) Spin-dependent DOS in Fe electrodes for zero and finite bias voltage. Vertical lines represent the left and right interfaces. The two spin channels correspond to transmission between inner–inner and outer–outer states. (b) Potential profiles of asymmetric MTJs under negative and positive bias voltage. Negative (positive) bias decreases (increases) the barrier transparency.

asymmetric bias dependence of TMR and TMR sign inversion at high bias were observed. For example, to model the NiO/MgO composite barrier, we choose $\varepsilon_{B_R} = 9.0$ eV, the same as the bulk, and $\varepsilon_{B_L} = 7.0$ eV, because the band gap of NiO is smaller compared to MgO. The calculated bias dependence of TMR is shown in figure 4. TMR is symmetric for unmodified MgO barriers. The insertion of a thin NiO layer at the left interface introduces asymmetry in the bias dependence of TMR. Thus, for positive (negative) bias higher (lower) voltage is required to change the sign of TMR. However, placing the NiO layer inside the MgO barrier essentially restores the symmetry in the bias dependence of TMR. When the NiO layer is at the interface t_L is different from t_R, resulting in asymmetric bias dependence of TMR. However a slight shift of the NiO layer from the interface yields $t_L = t_R$ and almost negligible asymmetry of TMR comes only through the asymmetric weighting with the S-matrix in the integral. Thus, the observed bias dependence and inversion of TMR can be understood simply in terms of asymmetric ITFs and the exchange bias in the electrodes.

Further on, the model can be used to explain the bias dependence of TMR in MTJs with metallic interface layers, such as Fe/Cr/MgO/Fe [10] and Fe/Fe_3O_4/MgO/CoMTJs [11]. We model metallic layers by lowering the onsite energy of the interface layer $\varepsilon_{B_L} < 6.0$ eV in which case the band crosses the Fermi level. The results for TMR are shown in figure 5

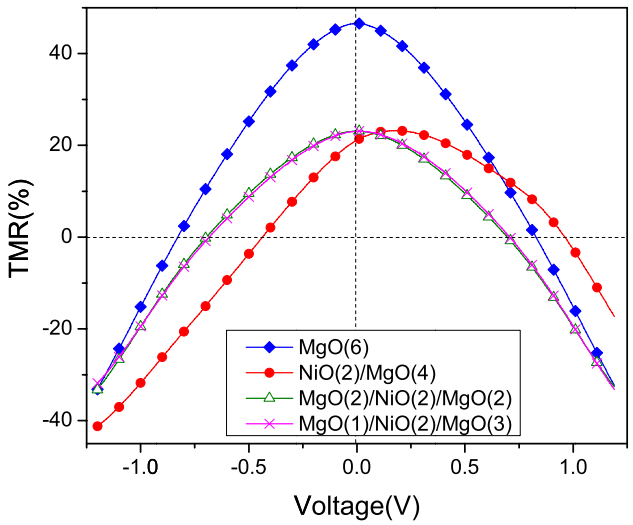

Figure 4. Bias dependence of TMR in CoFe/MgO/CoFe and CoFe/NiO/MgO/CoFe MTJs. The total barrier thickness is six monolayers for all curves. Black curve is for CoFe/MgO/CoFe MTJs. Green, blue and red curves are for CoFe/NiO/MgO/CoFe MTJs where the thickness of NiO is two monolayers. NiO is at the left interface (green curve), one/two monolayers away from the left interface towards the center of the barrier (red/blue curve).

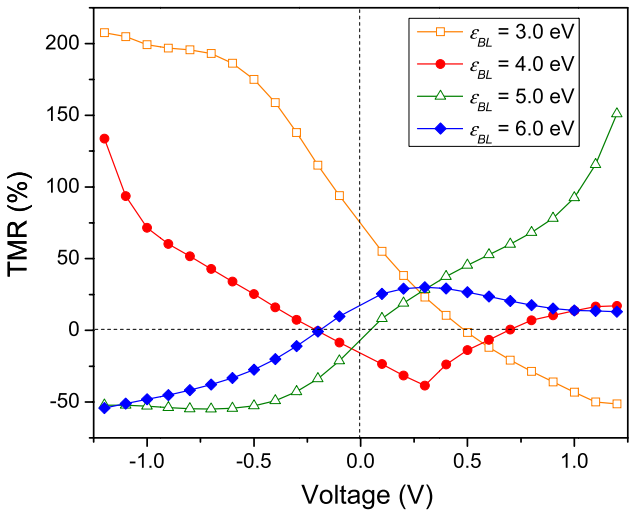

Figure 5. Bias dependence of TMR in MTJs in the resonant regime with a metallic layer of one monolayer thickness at the left interface. The total barrier thickness is eight monolayers.

for several voltages. In the tunneling regime TMR ($\varepsilon_{B_L} = 6.0$ eV) has the 'usual' form, with a maximum close to zero voltage and behaving as an even function of the voltage. For a shallow potential well at the interface ($\varepsilon_{B_L} = 5.0$ eV) the bias dependence of TMR already shows qualitatively different behavior; TMR inversion cannot be achieved by applying positive voltage. In this case we notice the interesting feature that TMR becomes an odd function of the bias. This suggests a possibility of combining memory and logic functions in the same bit [43, 44]. Moreover, TMR increases with voltage. In general memory stacks are operated at low voltage because TMR has a maximum. This feature could allow memories to be operated at higher voltage. Similar behavior but with reverse sign is observed for $\varepsilon_{B_L} = 3.0$ eV. Finally, for $\varepsilon_{B_L} = 4.0$ eV TMR completely reverses its behavior. It is inverse at zero bias and increases with applied bias. Similar qualitative behavior was observed experimentally in $Fe/Fe_3O_4/MgO/Co$ MTJs [11].

These features can be explained by the appearance of resonance states in the potential well created by the metallic layer at the interface which contribute to resonant tunneling [45]. In this regime it becomes possible that $|1 - g_{aa}\Sigma_L^\sigma| \approx 0$ for some combinations of E and $\boldsymbol{k}_\parallel$. The position of the resonance also depends parametrically on ε_{B_L}. At resonance, the ITF at the left interface $t_L^\sigma = \rho_L^\sigma D_L^\sigma$ will be strongly enhanced. The behavior of the TMR with voltage will depend on the way resonances overlap with the DOS of the electrodes.

To illustrate this we plot, in figure 6, the zero bias $\boldsymbol{k}_\parallel$-resolved DOS for the electrode (representative of t_R) and the first barrier layer for $\varepsilon_{B_L} = 3.0$ and $\varepsilon_{B_L} = 4.0$ eV (representative of t_L). In both cases there is one resonance in each spin channel. For $\varepsilon_{B_L} = 3.0$ eV the resonance overlaps with the majority DOS but it does not with the minority DOS. Thus, the term $t_L^\uparrow t_R^\uparrow$ gives the largest contribution to current and there is only non-resonant transmission in the AP configuration. Thus, $I_P > I_{AP}$ and TMR is positive. For $\varepsilon_{B_L} = 4.0$ eV the minority resonance starts to overlap with the electrode DOS, which results in very strong AP transmission, $I_{AP} > I_P$, and TMR becomes negative. As ε_{B_L} increases the resonances disappear altogether and we have a transition to the insulating regime at $\varepsilon_{B_L} = 6$ eV. Conversely for lower ε_{B_L} or for thicker interface more than one resonance can appear.

4. Conclusions

We report asymmetric bias dependence of TMR and TMR reversal at large bias in single crystal Fe/MgO-based MTJs: one with two morphologically different interfaces and one with a layer of O inserted at the bottom interface. We develop a model to describe the TMR behavior in MTJs with modified barriers, with the added benefit that it allows us to reinterpret and categorize the wide variety of experimental results. The model, although simple, captures the essential physics of the Fe/MgO-based MTJs (namely the Δ_1 filtering) and agrees qualitatively with the experimental data. It predicts two distinct regimes: tunneling when the modified interfaces are insulating, and resonant when the interfaces become metallic. In the tunneling regime, we observe asymmetric bias dependence of the TMR resulting from the asymmetry of the ITFs due to the difference of the morphology of the interfaces. We explain the TMR inversion results from the realignment of the electrode DOS in large bias, which overcomes the exchange splitting in the electrodes. In the resonant regime, the electron tunneling through the resonant levels at the interface can dominate the transmission probability for a particular spin channel. Judicious choices of the position of the resonant level allow for control of the shape of the TMR bias dependence. We have demonstrated cases of normal TMR decreasing with bias, inverse TMR increasing with bias and TMR changing sign for positive and negative bias.

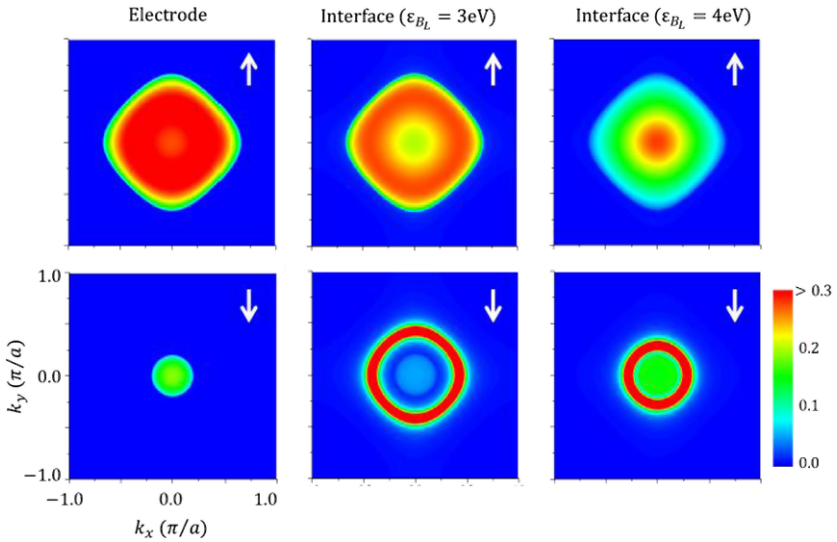

Figure 6. $k_{\|}$-resolved majority and minority DOS in the electrodes (left panels), and induced DOS in the first barrier layer at the left interface for $\varepsilon_{B_L} = 3$ eV (middle panels) and $\varepsilon_{B_L} = 4$ eV (right panels).

Acknowledgments

The work at the University of Puerto Rico was supported by NSF (Grants Nos EPS-1002410, EPS-1010094, and DMR-1105474) and DOE (Grant No. DE-FG02-08ER46526). P-J Zermatten, G Gaudin, F Bonell, S Andrieu, and C Tiusan acknowledge the SPINCHAT project ANR-07-BLAN-341. C Tiusant acknowledges POS CCE ID. 574, code SMIS-CSNR 12467.

References

[1] Fert A *et al* 2001 Review of recent resultson spin polarized tunneling and magnetic switching by spin injection *Mater. Sci. Eng.* B **84** 1–9
[2] Butler W H, Zhang X G and Schulthess T C 2001 Spin-dependent tunneling conductance of Fe|MgO|Fe sandwiches *Phys. Rev.* B **63** 054416
[3] Yuasa S, Nagahama T, Fukushima A, Suzuki Y and Ando K 2004 Giant room-temperature magnetoresistance in single-crystal Fe/MgO/Fe magnetic tunnel junctions *Nature Mater.* **3** 868–71
[4] Parkin S S P, Kaiser C, Panchula A, Rice P M, Hughes B, Samant M and Yang S-H 2004 Giant tunneling magnetoresistance at room temperature with MgO (100) tunnel barriers *Nature Mater.* **3** 862–7
[5] Ikeda S, Hayakawa J, Ashizawa Y, Lee Y M, Miura K, Hasegawa H, Tsunoda M, Matsukura F and Ohno H 2008 Tunnel magnetoresistance of 604% at 300 K by suppression of Ta diffusion in CoFeB/MgO/CoFeB pseudo-spin-valves annealed at high temperature *Appl. Phys. Lett.* **93** 082508
[6] Tsymbal E, Belashchenko K, Velev J, Jaswal S S, van Schilfgaarde M, Oleynik I I and Stewart D A 2007 Interface effects in spin-dependent tunneling *Prog. Mater. Sci.* **52** 401–20
[7] Velev J P, Dowben P A, Tsymbal E Y, Jenkins S J and Caruso A N 2008 Interface effects in spin-polarized metal/insulator layered structures *Surf. Sci. Rep.* **63** 400–25
[8] Sharma M, Wang S X and Nickel J H 1999 Inversion of spin polarization and tunneling magnetoresistance in spin-dependent tunneling junctions *Phys. Rev. Lett.* **82** 616
[9] Yang H, Yang S H, Qi D C, Rusydi A, Kawai H, Saeys M, Leo T, Smith D J and Parkin S S P 2011 Negative tunneling magnetoresistance by canted magnetization in MgO/NiO tunnel barriers *Phys. Rev. Lett.* **106** 167201
[10] Greullet F, Tiusan C, Montaigne F, Hehn M, Halley D, Bengone O, Bowen M and Weber W 2007 Evidence of a symmetry-dependent metallic barrier in fully epitaxial MgO based magnetic tunnel junctions *Phys. Rev. Lett.* **99** 187202
[11] Greullet F, Snoeck E, Tiusan C, Hehn M, Lacour D, Lenoble O, Magen C and Calmes L 2008 Large inverse magnetoresistance in fully epitaxial Fe/Fe_3O_4/MgO/Co magnetic tunnel junctions *Appl. Phys. Lett.* **92** 053508
[12] Guerrero R, Herranz D, Aliev F G, Greullet F, Tiusan C, Hehn M and Montaigne F 2007 High bias voltage effect on spin-dependent conductivity and shot-noise in carbon-doped Fe(001)/MgO(001)/Fe(001) magnetic tunnel junctions *Appl. Phys. Lett.* **91** 132504
[13] Tiusan C, Sicot M, Hehn M, Belouard C, Andrieu S, Montaigne F and Schuhl A 2006 Fe/MgO interface engineering for high-output-voltage device applications *Appl. Phys. Lett.* **88** 062512
[14] Bonell F, Andrieu S, Bataille A M, Tiusan C and Lengaigne G 2009 Consequences of interfacial Fe–O bonding and disorder in epitaxial Fe/MgO/Fe(001) magnetic tunnel junctions *Phys. Rev.* B **79** 224405
[15] Zermatten P-J, Bonell F, Andrieu S, Chshiev M, Tiusan C, Schuhl A and Gaudin G 2012 Influence of oxygen monolayer at Fe/MgO interface on transport properties in Fe/MgO/Fe(001) magnetic tunnel junctions *Appl. Phys. Express* **5** 023001
[16] Tiusan C, Vincent J F, Bellouard C, Hehn M, Jougelet E and Schuhl A 2004 Interfacial resonance state probed by spin-polarized tunneling in epitaxial Fe/MgO/Fe tunnel junctions *Phys. Rev. Lett.* **93** 106602
[17] Zermatten P-J, Gaudin G, Maris G, Miron M, Schuhl A, Tiusan C, Greullet F and Hehn M 2008 Experimental evidence of interface resonance states in single-crystal magnetic tunnel junctions *Phys. Rev.* B **78** 033301
[18] Du G X, Wang S G, Ma Q L, Wang Y, Ward R C C, Zhang X-G, Wang C, Kohn A and Han X F 2010 Spin-dependent tunneling spectroscopy for interface characterization of epitaxial Fe/MgO/Fe magnetic tunnel junctions *Phys. Rev.* B **81** 064438

[19] Ando Y, Miyakoshi T, Oogane M, Miyazaki T, Kubota H, Ando K and Yuasa S 2005 Spin-dependent tunneling spectroscopy in single-crystal Fe/MgO/Fe tunnel junctions *Appl. Phys. Lett.* **87** 142502
[20] Jullière M 1975 Tunneling between ferromagnetic films *Phys. Lett.* A **54** 225–6
[21] Zhang C, Zhang X-G, Krstic P S, Cheng H-P, Butler W-H and MacLaren J M 2004 Electronic structure and spin-dependent tunneling conductance under a finite bias *Phys. Rev.* B **69** 134406
[22] Heiliger C, Zahn P, Yavorsky B Y and Mertig I 2005 Influence of the interface structure on the bias dependence of tunneling magnetoresistance *Phys. Rev.* B **72** 180406(R)
[23] Heiliger C, Zahn P, Yavorsky B Yu and Mertig I 2006 Interface structure and bias dependence of Fe/MgO/Fe tunnel junctions: *ab initio* calculations *Phys. Rev.* B **73** 214441
[24] Waldron D, Timoshevskii V, Hu Y, Xia K and Guo H 2006 First principles modeling of tunnel magnetoresistance of Fe/MgO/Fe trilayers *Phys. Rev. Lett.* **97** 226802
[25] Tiusan C, Greullet F, Hehn M, Montaigne F, Andrieu S and Schuhl A 2007 Spin tunneling phenomena in single-crystal magnetic tunnel junction systems *J. Phys.: Condens. Matter.* **19** 165201
[26] Belashchenko K D, Velev J and Tsymbal E Y 2005 Effect of interface states on spin-dependent tunneling in Fe/MgO/Fe tunnel junctions *Phys. Rev.* B **72** 140404(R)
[27] Zhang X-G, Butler W H and Bandyopadhyay A 2003 Effects of the iron-oxide layer in Fe–FeO–MgO–Fe tunneling junctions *Phys. Rev.* B **68** 092402
[28] Bonell F, Andrieu S, Tiusan C, Montaigne F, Snoeck E, Belhadji B, Calmels L, Bertran F, Le Fevre P and Taleb-Ibrahimi A 2010 Influence of misfit dislocations on the magnetoresistance of MgO-based epitaxial magnetic tunnel junctions *Phys. Rev.* B **82** 092405
[29] Stamenova M, Sanvito S and Todorov T N 2005 Current-driven magnetic rearrangements in spin-polarized point contacts *Phys. Rev.* B **72** 134407
[30] Yang H X, Chshiev M, Kalitsov A, Schuhl A and Butler W H 2010 Effect of structural relaxation and oxidation conditions on interlayer exchange coupling in Fe|MgO|Fe tunnel junctions *Appl. Phys. Lett.* **96** 262509
[31] Raza T and Raza H 2011 Independent-band tight-binding parameters for Fe–MgO–Fe magnetic heterostructures *IEEE Trans. Nanotechnol.* **10** 237–43
[32] Theodonis I, Kalitsov A, Kioussis N, Chshiev M and Butler W H 2006 Anomalous bias dependence of spin torque in magnetic tunnel junctions *Phys. Rev. Lett.* **97** 237205
[33] Chshiev M, Theodonis I, Kalitsov A, Kioussis N and Butler W H 2008 Voltage dependence of spin transfer torque in magnetic tunnel junctions *IEEE Trans. Magn.* **44** 2543–6
[34] Kalitsov A, Chshiev M, Theodonis I, Kioussis N and Butler W H 2009 Spin-transfer torque in magnetic tunnel junctions *Phys. Rev.* B **79** 174416
[35] Khalil A H, Stiles M D and Heiliger C 2010 Influence of band parameters on spin-transfer torque in tunnel junctions: model calculationds *IEEE Trans. Magn.* **46** 1745–7
[36] Kalitsov A, Silvestre W, Chshiev M and Velev J 2013 Spin torque in magnetic tunnel junctions with asymmetric barriers *Phys. Rev.* B **88** 104430
[37] Caroli C, Combescot R, Nozieres P and Saint-James D 1971 Direct calculations of the tunneling current *J. Phys. C: Solid State Phys.* **4** 916–29
[38] Meir Y and Wingreen N S 1992 Landauer formula for the current through an interacting electron region *Phys. Rev. Lett.* **68** 2512
[39] Chang Y C and Schulman J N 1982 Complex band structures of crystalline solids: an eigenvalue method *Phys. Rev.* B **25** 3975
[40] Zhang X-G and Butler W H 2003 Band structure, evanescent states, and transport in spin tunnel junctions *J. Phys.: Condens. Matter* **15** R1603
[41] Belashchenko K D, Tsymbal E Y, van Schilfgaarde M, Stewart D A, Oleynik I I and Jaswal S S 2004 Effect of interface bonding on spin-dependent tunneling from the oxidized Co surface *Phys. Rev.* B **69** 174408
[42] Faleev S V, Mryasov O N and van Schilfgaarde M 2012 Effect of correlations on electronic structure and transport across (001) Fe/MgO/Fe junctions *Phys. Rev.* B **85** 174433
[43] Binek C and Doudin B 2005 Magnetoelectronics with magnetoelectrics *J. Phys.: Condens. Matter* **17** L39
[44] Chen X, Hochstrat A, Borisov P and Kleemann W 2006 Magnetoelectric exchange bias systems in spintronics *Appl. Phys. Lett.* **89** 202508
[45] Tang Y-H, Kioussis N, Kalitsov A, Butler W H and Car R 2009 Controlling the nonequilibrium interlayer exchange coupling in asymmetric magnetic tunnel junctions *Phys. Rev. Lett.* **103** 057206